



Vaasan yliopisto
UNIVERSITY OF VAASA

OSUVA Open
Science

This is a self-archived – parallel published version of this article in the publication archive of the University of Vaasa. It might differ from the original.

Energy storage systems implementation and photovoltaic output prediction for cost minimization of a Microgrid

Author(s): Rajamand, Sahbasadat; Shafie-khah, Miadreza; Catalao, Joao P.S.

Title: Energy storage systems implementation and photovoltaic output prediction for cost minimization of a Microgrid

Year: 2022

Version: Accepted manuscript

Copyright ©202X Elsevier. This manuscript version is made available under the Creative Commons Attribution–NonCommercial–NoDerivatives 4.0 International (CC BY–NC–ND 4.0) license, <https://creativecommons.org/licenses/by-nc-nd/4.0/>

Please cite the original version:

Rajamand, S., Shafie-khah, M. & Catalao, J. P.S. (2022). Energy storage systems implementation and photovoltaic output prediction for cost minimization of a Microgrid. *Electric Power Systems Research* 202, 107596. <https://doi.org/10.1016/j.epsr.2021.107596>

Energy Storage Systems Implementation and Photovoltaic Output Prediction for Cost Minimization of a Microgrid

Sahbasadat Rajamand¹, Miadreza Shafie-khah², João P.S. Catalão^{3,*}

¹ *Department of Electrical Engineering, Kermanshah Branch, Islamic Azad University, Kermanshah, Iran*

² *School of Technology and Innovations, University of Vaasa, Vaasa, Finland*

³ *Faculty of Engineering of the University of Porto and INESC TEC, Porto, Portugal*

**catalao@fe.up.pt*

Abstract: Energy storage system (ESS) has great importance in saving energy in new power systems. Optimum selection of these elements poses a new challenge to improve the energy management and prevent cost increases in the system. Also, renewable energy resources have been increasingly used in microgrids. The uncertainty and variation of renewable distributed generation (DG) affect the performance of power systems. In this paper, ESS implementations and photovoltaic (PV) power prediction are used to improve voltage/power profile of the system and reduce the total cost of the microgrid. The purpose of this paper is the optimal installation of ESSs in a microgrid to minimize the total cost where quantile nearest neighbour forecasting is utilized for PV output power prediction as an efficient approach. Gathering data of the last samples in time duration can be used for an effective prediction of PV output in this method, which can overcome PV uncertainty due to changes in solar irradiation and other parameters. Artificial neural networks combined with multi-layer perceptron and genetic algorithm are used for optimizing the size and location of ESSs in the system. Simulation results show that the proposed method improves the power profile as 14%, 21% and 28%, relatively to the scenarios of optimal ESS installation without PV prediction, using PV prediction but with no optimal ESS implementation and not using PV- no ESS implementation, respectively. Moreover, the accuracy of the proposed prediction method is more than the gradient-descent and RNN methods by about 12% and 5%, respectively, as shown in the simulation results. Also, the cost reduction of proposed method is enhanced as 24% and 31% relatively to the cases of optimal ESS installation without PV prediction and PV prediction without optimal ESS implementation, respectively.

Keywords— Energy storage systems; microgrids; uncertainty; distributed generation; photovoltaic power.

Nomenclature

Index

Act	Actual
b, b'	Index of buses
C	Capacity
Ch	Charge
Dch	Discharge
E	Energy
ESS	Energy storage system
F	Forecast

K	Number of Step times
N	Number of elements
Nom	Nominal value
P	Power
PV	Photo-Voltaic
QNN	Quantile nearest neighbour
LWMA	linear weighted moving average
<i>card</i>	cardinality operator
+	Charging status
-	Discharging status
Parameters	
b_s^+	Storage charging state
b_s^-	Storage discharging state
b_s^{Max}	Maximum storage charging state
FF	Fitness Function
N_{ESS}	Number of ESS
N_G	Number of diesel generators
N_{PV}	Number of PV generators
β	Charge-discharge efficiency
Variables	
C^{Ch}	Capacity of charge
C^{Dch}	Capacity of discharge
C_n^{ESS}	Capacity of storage
$C_n^{ESS,Min}$	Minimum of storage capacity
$C_n^{ESS,Max}$	Maximum of storage capacity
E_n^{ESS}	Storage energy
$E_{n,\Delta t}^{ESS}$	Storage energy in time step Δt
E^G	Diesel Generator energy
E^{Load}	Load energy
E^{LOSS}	Energy loss
E^{PV}	PV energy
I,I2	Current flow, Squared current flow
$I_{b,b'}^{Max}$	Maximum current between buses
p^{Ch}	Charge power
p^{DCh}	Discharge power
$p_{n,t,sc}^{Ch,ESS}$, $p_{n,t,sc}^{Dch,ESS}$	Charging and discharging power of ESS
p_n^{ESS}	Power of ESS
$p_n^{ESS,Min}$	Minimum of storage power
$p_n^{ESS,Max}$	Maximum of storage power
$P_{b,t,sc}^G$	Power generation of Diesel Generator unit
$p^{G,Nom}$	Nominal Diesel Generator power
$p_{b,t,sc}^{Load}$	Electric active load at bus b

$P_{b,t,sc}^{PV}$	Power generation of PV unit
P_{act}^{PV}	Actual PV power
P_f^{PV}	Forecasted PV power
$P_{Sb,t,sc}^{Wh}$	The injected power from upper grid
P^+	Active power flows in downstream directions
P^-	Active power flows in upstream directions
$Q_{n,t,sc}^{ch,ESS}, Q_{n,t,sc}^{Dch,ESS}$	Charging and discharging reactive power of ESS
$Q_{b,t,sc}^G$	Reactive power generation of Diesel Generator unit
$Q_{b,t,sc}^{Load}$	Electric reactive load at bus b
$Q_{Sb,t,sc}^{PV}$	Reactive power generation of PV unit
$Q_{Sb,t,sc}^{Wh}$	The injected reactive power from upper grid
Q^+	Reactive power flows in downstream directions
Q^-	Reactive power flows in upstream directions
$R_{b,b}, X_{b,b}$	Distribution lines resistance and reactance
V	Voltage
$V_{Max}, V_{Min}, V^{Nom}$	Maximum, minimum, and nominal voltage
w	Weight vector
x	Input vector of neural network
ε	Error
ε^{PV}	PV power prediction error
$(\sigma^2)^{PV}$	Variance of PV power prediction error
Δt	Time step
ΔS	Upper limit in the discretization of quadratic flow (kVA).
λ_n^{Ess}	Cost of ESS (\$/kWh)
λ_n^G	Cost of Diesel Generator(\$/kWh)
λ_n^{PV}	Cost of PV (\$/kWh)
\hat{P}_q	forecasted quantile PV power
P_q	observed previous data
$P_{q,opt}$	optimum observed previous data
$\mu_{pv,err}$	mean of normal distribution of prediction error
L_v	voltage coefficients of PV module
L_i	current coefficients of PV module
$temp_{panel}$	PV panel temperature
$B_{m.t.irr}$	function of irradiation
$\beta_{t.irr}$	efficiency of irradiation transfer
ρ_t	outage probability function

1. Introduction

Using the Energy Storage System (ESS) can be a crucial solution for reducing the required energy generation in the power system. ESS can save the energy in off-peak times and compensate for the shortage of energy for load supporting in on-peak times [1]. Using ESS can improve the reliability of the system in load supporting and DG planning. In addition, due to uncertainty of renewable DGs such as photovoltaic (PV) and wind turbine (WT), it is necessary to predict the output power to prevent underestimation of loads and DG generation/planning. Thus, to overcome these challenges, ESS installation and PV prediction model is used to improve the power/voltage profile and reduce the cost of the system.

ESS reduces the fluctuations of voltage and power of the system and hence increases the reliability and stability of the system [1-3]. Various forms of energy storage systems such as capacitive energy storage, thermal energy storage and battery can be used in power systems [4-6]. Optimal multi-objective scheduling of combined heat-power (CHP)-based microgrid is proposed in [7] including compressed air energy storage (CAES), renewable energy sources and thermal energy storage. Cost reduction and exploiting the wasted heat energy to supply the loads in emergency condition are some advantages of this method.

In this paper, the optimization method which is based on epsilon-constraint technique is presented using fuzzy decision making to achieve the optimal selection from all the Pareto solutions. In [8], the usage of EVs and EVCS as energy storage units and optimal strategy of charging/discharging considering the distribution network constraints is presented to reduce the total cost and improvement performance where the scheduling is done in 24 hours. In [9], conditional value at risk (CVaR)-based random method is proposed to compensate the uncertainty of WT by using hydrogen storage system associated with wind power production. Handling the risk and compensating the uncertainty are the results of this method.

Note that it is not possible to implement ESS in all buses and therefore, the location and capacity of the ESS are important in the system design [10]. It is worth mentioning that ESS implementation costs must be considered and compared to the cost reduction of energy generation due to ESS existing which concludes the justification of ESS implementation. Optimal ESS implementation in terms of location and size must be performed by the evolutionary algorithms based on minimizing of the cost function. Using this optimal installation of ESS (optimal sizes in optimal locations of the system) results in cost reduction, voltage/power profile improvement and more reliability in load supporting and load balance.

In another side, renewable energies are increasingly used in new power systems as efficient power resources [11]. PV or WT can support the main part of the system load and help the stability of the system. The main challenge of these renewable resources is the uncertainty of power generation [12, 13]. The generated power from PV is non-deterministic and thus, it can be assumed as a stochastic random process. Moreover, the PV power fluctuation due to the solar radiation and temperature fluctuations affects the microgrid system operation and costs. Therefore, this subject causes the researchers to focus on approaches for forecasting the PV output power. The forecasting methods are used to predict the output power of the PV systems, which is valuable in terms of the technical and economical points of view [14]. PV output is affected by many factors such as solar radiation, temperature, humidity, dust, rain, and so on. Thus, prediction of PV generation depends on these parameters to obtain the accurate model of prediction and hence, the performance of the system is noticeably improved. In [15], uncertainty of PV/WT and its effect on performance of microgrid is discussed where a new retail electricity pricing method based on CVaR optimization framework is suggested to reduce the effects of risk of unpredictable renewable energy sources. In this paper, the energy planning of the next day in microgrid is done.

Optimal ESS implementation in [16] based on optimum size and location is discussed while no power forecasting is mentioned. In [17], a prediction method is applied for PV output power but forecasting error is not considered. Both stochastic WT power and load demand are assumed in [18] where Monte-Carlo sampling of the distributions (assumed as Normal distribution at each time-step) is used to determine the optimal storage capacity related to certain reliability index taking into account one-day historical data.

Energy management and cost reduction based on demand response in the multiple microgrids is proposed in [19] to tackle the challenges associated with demand response programs to prevent rebound peaks. Two-stage hybrid stochastic-information gap-decision theory (IGDT) is proposed in [20] based on joint energy and flexible ramping reserve in CHP-based systems. The uncertainties of load demands and WT are considered based on Monte Carlo simulation method to be compensated in the system. Probabilistic multi-stage optimization framework with depth analysis using appliance model, consumer operation and AC grid considering weather and load demand uncertainty is suggested in [21, 22]. Electricity access specially in developing countries is the main goal of these papers.

Focusing on prediction part, artificial neural network (ANN) can be selected as an efficient tool for this purpose. ANN computation ability can be used for the prediction of many scientific events such as PV output power in [23]. Data were measured and recorded for one complete year in this study. The use of neural network for the prediction of PV output power is also discussed in some papers as [24-27]. Many works have been concentrated on improving the prediction accuracy of ANN architectures [28-30]. Short-term forecasting and recurrent neural network are discussed in these papers. In [31], multi-layer perceptron (MLP) ANN is used to accurately predict the power of a PV system because of its ability in updating the weights of the network. In [32], SVM is used to predict the PV output power with interesting result.

Due to above, many papers have been focused on the challenges of optimal ESS implementation and accurate PV output power prediction. In this paper, both challenges have been considered to minimize the cost of energy generation in power grid. To achieve this goal, the cost function is generated including the cost of diesel-generator, PV and ESS elements. To achieve more precise prediction that affects the cost profile of the system, the quantile nearest neighbour (QNN) forecasting is used to predict the next data based on the regression and prediction error minimization. A window of last N_q samples is used in this approach which offers N_q -order prediction strategy to obtain more precise prediction. Then multi-layer perceptron artificial neural network (MLP-ANN) is used for training and testing of the forecasted data.

ANN is assumed as the supervised network and some parts of data are used for training and other parts are used for test of the network. The effective input parameters in PV output power are completely assumed for more accurate prediction which are fed to ANN. These parameters are assumed as temperature, humidity, dust, irradiation of solar, angle of radiation, the surface of the panel, air pressure, and the panel efficiency in energy conversion. Due to the various parameters and the complexity of weight updating, genetic algorithm (GA) is applied for obtaining the optimum weights of the ANN in the proposed method. To the best authors' knowledge, the analysis of ESS implementation and PV output prediction using QNN, MLP-ANN and GA for cost minimization of a microgrid has not been addressed in the literature. A taxonomy table is provided to more highlight the novelties of this paper compared to other related papers.

Table 1: Taxonomy table (comparison of proposed work to other related efficient works in the literature)

Reference	PV	ESS	WT	PV power prediction	WT power prediction	ESS implementation optimization (size)	ESS implementation optimization (location)	Cost minimization	Power profile	Neural network	GA	Fuzzy-based algorithm	Statistical method	Electric demand (uncertainty)
[14]	✓	✓		✓					✓					
[16]	✓	✓		✓					✓				✓	
[17]		✓				✓	✓	✓						✓(✓)
[18]		✓	✓		✓	✓		✓	✓					✓
[23]	✓			✓						✓				
[24]	✓			✓								✓		
[25]	✓			✓						✓				
[27]	✓			✓				✓						✓(✓)
[26]	✓			✓				✓					✓	✓
[29]	✓			✓					✓	✓				
[31]	✓			✓						✓				
[42]	✓	✓		✓					✓					
[43]	✓	✓		✓		✓		✓	✓					
[44]	✓	✓		✓		✓	✓	✓					✓	
[45]	✓	✓		✓		✓	✓		✓	✓				
This paper	✓	✓		✓		✓	✓	✓	✓	✓	✓			✓(✓)

The novel contributions of the paper are summarized as follows:

- Optimal operation of the microgrid using ESS implementation and PV output prediction. PV output power is assumed as a stochastic process where its variance is applied in the cost function problem to consider the uncertainty. ESS optimization in size and location using the proposed evolutionary algorithm can enhance the performance of the microgrid.
- PV output power prediction using quantile nearest neighbour (QNN) forecasting and multilayer perceptron network. QNN forecasting is based on regression data and minimization of prediction error applied to MLP-ANN for training and testing approach. GA is used for updating weight coefficients in MLP-ANN and location/size optimization of ESS implementation.
- Complete describing of effective parameters on the PV output power and applying to the input vector of MLP-ANN. These effective parameters are temperature, humidity, dust, irradiation of solar, angle of radiation, the surface of the panel, air pressure, and the panel efficiency in energy conversion.
- Considering four scenarios based on using/not using of optimal ESS implementation and using/not using of proposed accurate PV power prediction and comparing of them in terms of voltage/power profile and total cost

The rest of the paper is as follows. In Section 2, problem formulation and discussion are presented while in Section 3, the proposed method is stated. In Section 4, simulation results are discussed and finally, some conclusions are drawn in Section 5.

2. Problem Formulation

In this section, the cost function is firstly defined to be minimized. The 24-hour model consisting of 2-hour steps is applied and analysed in the optimization process. The profiles of load, ESS and PV are considered in each 2-hour step and thus, 12 time steps are used for obtaining the cost profile of the system. For the total cost, one-year period is considered where the summation of one-day costs is applied in this time period. The function includes the cost of generated power from diesel generators, PV generators and also storage elements.

The cost function of 24-hour profile is described as below:

$$FF(one - day) = \sum_{k=1}^K \left(\sum_{n=1}^{N_G} \lambda_n^G P_n^G + \sum_{n=1}^{N_{ESS}} \lambda_n^{ESS} P_n^{ESS} + \sum_{n=1}^{N_{PV}} \lambda_n^{PV} ((\sigma_n^2)^{PV} P_n^{PV}) \right) \Delta t_k \quad (1)$$

where k denotes the step-time index for calculation of cost during the time interval of power grid. Obviously, for the one-year profile, we have:

$$FF(one - year) = \sum_{i=1}^{365} FF(one - day)_i \quad (2)$$

The goal of this paper is to reduce the total cost of the system using the ESS implementation on some buses and accurate PV output power prediction. In this minimization, precise PV power prediction can be used to achieve the mentioned purpose and compensate the PV-based uncertainty of the system which directly affects the total cost of the microgrid. This optimization can be performed subjected to several constraints as below:

$$P^G \leq P^{G,Nom} \quad (3)$$

$$bs^+ \leq \beta bs^{Max} \quad (4)$$

$$bs^- \leq (1 - \beta) bs^{Max} \quad (5)$$

$$C_n^{ESS,Min} < C_n^{ESS} < C_n^{ESS,Max} \quad (6)$$

$$C^{Ch} = C^{DCh} \quad (7)$$

$$|E^G + E^{PV} - E^{Load} - E^{Loss}| = E^{ESS} \quad (8)$$

$$P^{ESS} = \alpha P^{Ch} + (1 - \alpha) P^{DCh} \quad (9)$$

$$P_n^{ESS,Min} < P_n^{ESS} < P_n^{ESS,Max} \quad (10)$$

$$E_{\Delta t_1}^{ESS} = E_{\Delta t_K}^{ESS} \quad (11)$$

$$P_{Sb,t,sc}^{Wh} + P_{b,t,sc}^G + P_{b,t,sc}^{PV} + \sum_{ESS} P_{n,t,sc}^{DCh,ESS} - \sum_{ESS} P_{n,t,sc}^{Ch,ESS} \quad (12)$$

$$+ \sum_{b' \in B} [(P_{t,b,b'}^+ - P_{t,b,b'}^-)]$$

$$- \sum_{b' \in B} [(P_{t,b,b'}^+ - P_{t,b,b'}^-) + R_{b,b'} I_{2,t,b,b'}]$$

$$= P_{b,t,sc}^{Load} \quad \forall t, \forall b.$$

$$Q_{Sb,t,sc}^{Wh} + Q_{b,t,sc}^G + Q_{b,t,sc}^{PV} + \sum_{ESS} Q_{n,t,sc}^{DCh,ESS} - \sum_{ESS} Q_{n,t,sc}^{Ch,ESS} \quad (13)$$

$$+ \sum_{b' \in B} [(Q_{t,b,b'}^+ - Q_{t,b,b'}^-)]$$

$$- \sum_{b' \in B} [(Q_{t,b,b'}^+ - Q_{t,b,b'}^-) + X_{b,b'} I_{2,t,b,b'}]$$

$$= Q_{b,t,sc}^{Load} \quad \forall t, \forall b.$$

$$(P_{t,b,b'}^+ + P_{t,b,b'}^-) \leq V^{Nom} I_{b,b'}^{max} \quad \forall t, \forall b. \quad (14)$$

$$(Q_{t,b,b'}^+ + Q_{t,b,b'}^-) \leq V^{Nom} \times I_{b,b'}^{max} \quad \forall t, \forall b. \quad (15)$$

$$V2_{t,b} - 2R_{b,b'}(P_{t,b,b'}^+ - P_{t,b,b'}^-) - 2X_{b,b'}(Q_{t,b,b'}^+ - Q_{t,b,b'}^-) \quad (16)$$

$$- (R_{b,b'}^2 + X_{b,b'}^2)I2_{t,b,b'} - V2_{t,b'} = 0 \quad \forall t, \forall b.$$

$$V2_{t,b}^{Nom} I2_{t,b,b'} = \sum_{\tau} (2\tau - 1) \Delta S_{t,b,b'} \Delta P_{t,b,b'} \quad (17)$$

$$+ \sum_{\tau} (2\tau - 1) \Delta S_{t,b,b'} \Delta Q_{t,b,b'} \quad \forall t, \forall b.$$

$$P_{t,b,b'}^+ + P_{t,b,b'}^- = \sum_{\tau} \Delta P_{t,b,b'}(\tau) \quad \forall t, \forall b. \quad (18)$$

$$Q_{t,b,b'}^+ + Q_{t,b,b'}^- = \sum_{\tau} \Delta Q_{t,b,b'}(\tau) \quad \forall t, \forall b. \quad (19)$$

$$\Delta P_{t,b,b'}(\tau) \leq \Delta S_{t,b,b'} \quad , \quad \Delta Q_{t,b,b'}(\tau) \leq \Delta S_{t,b,b'} \quad \forall t, \forall b. \quad (20)$$

$$I2_{t,b,b'} \leq (I_{b,b'}^{Max})^2 \quad \forall t, \forall b. \quad (21)$$

$$V_{Min}^2 \leq V2 \leq V_{Max}^2 \quad \forall t, \forall b. \quad (22)$$

$$V2_{t,b}^{Nom} = (V^{Nom})^2 \quad \forall t, \forall b. \quad (23)$$

$$\Delta S_{t,b,b'} = \frac{V^{Nom} I_{b,b'}^{Max}}{\tau} \quad \forall t, \forall b. \quad (24)$$

$$P_{t,b}^{\bar{u}} \tan(\cos^{-1}(-\theta)) \leq Q_{t,b}^{\bar{u}} \leq P_{t,b}^{\bar{u}} \tan(\cos^{-1}(\theta)) \quad \forall t, \forall b. \quad (25)$$

$$E^{ESS,t+1} = E^{ESS,t} + \int_t^{t+1} P^{ESS,u} du \quad (26)$$

where constraint (3) describes that the diesel generated power is up to the rated value. The charge state of ESS is bounded to the maximum of storage in (4) and also it is set for discharge state in (5). Combining of (4) and (5) shows the non-simultaneous charge and discharge of ESS in which β represents the efficiency of charge-discharge operation. Constraint (6) states that capacity of storage is between minimum and maximum value of existing devices capacity. In this paper, maximum and minimum values are 0.9 and 0.1 of the storage capacity, respectively. Also, the total storage capacity of charge must be equal to the total discharge capacity for all storage elements (Eq. 7). Constraint (8) states that the generated energy from diesel and PV minus the consumed in load and loss is equal to the storage energy. Indeed, the total generated power subtracted by the loss and load demand can be stored in storage units. Moreover, if the inside of absolute sign in the left side of this equation is lower than zero, the system must use the discharge state of ESS to support the extra demand power. Obviously, in the extra power generation, the ESS can be charged. Eq. (9) also mentions the total storage equals the combination of charging and discharging with weighting coefficients of α and $(1 - \alpha)$ determined due to bs^+ and bs^- . Eq. (10) states that the power of ESS is limited to its maximum and minimum value. Finally, the Eq. (11) presents that the initial storage energy in the first time step is equal to the storage energy in the last time step for the cyclic analysis of the optimization problem. Equations (12)-(13) describe the power balance for both active and reactive power considering all units in the microgrid. The bound on active and reactive power due to nominated voltage are presented in Equations (14) -(15) while equation

(16) presents the voltage balance in the buses due to input or output power of buses. Linearization of branch power flow is done for radial networks in equations (17) – (24). Linearized active and reactive power is performed in (17). Piecewise linearization of constraints is denoted in (18) – (24) [33, 34]. The constraint related to the power factor is stated in (25) where in (26), the energy updating of ESS in each time-step is presented. In all constraints, it must be noted that charging and discharging cannot be occurred simultaneously and because of that, the variables bs^- and bs^+ are used for the charge and discharge states, respectively.

3. Proposed Method

In Eq. (1), all parameters and variables are deterministic except the PV generated power. PV generated power is stochastic and depends on solar radiation, temperature, humidity, dust, rain, and so on. Thus, this parameter is weighted by $(\sigma_n^2)^{PV}$ that is the variance of PV power generation. Accurate prediction of PV generated power in time interval analysis of the system can significantly influence on the cost reduction. Moreover, using the optimal ESS implementation in this system can efficiently improve the cost and performance. In this paper, QNN is used for PV output power forecasting. The method is described as:

$$\hat{P}_q = f(\mathbf{x}, P_q) \quad (27)$$

where \hat{P}_q is represented for forecasted quantile PV power, \mathbf{x} is the vector of input and P_q is the observed previous data. The role of the function of forecasting ($f(\cdot)$) must be allocated to minimize the prediction error. One of the best option is linear combination of previous observations and input parameters with different weights known as linear weighted moving average (LWMA). To select the related previous samples, nearest neighbour strategy based on quantile regression method is stated as:

$$\begin{aligned} P_{q,opt} &= \operatorname{argmax} \operatorname{card}\{H_n\} \quad (28) \\ \text{s.t. } H_n: \max\{d(p_i, p_j)\} &\leq \min\{\min\{d(p_i, p_j)\}, \varepsilon_{Th}\} \\ \operatorname{card}\{H_n\} &\leq N_q \\ H_n^{pref} &= H_{n,opt} \end{aligned}$$

where card is the cardinality operator. Thus the vector of predicted data for training set is described as:

$$P_q = [P_{q,1}, P_{q,2}, \dots, P_{q,N_q}] \quad (29)$$

The criteria on which the best samples chosen and the minimum regression data can be achieved can be stated as:

$$\begin{aligned} Q_{p,q} &= \frac{1}{N_q} \sum_{n=1}^{N_q} \begin{cases} (q-1) \cdot (\hat{P}_n - f(\mathbf{x}, P_q)) & \hat{P}_n < f(\mathbf{x}, P_q) \\ (q) \cdot (\hat{P}_n - f(\mathbf{x}, P_q)) & \text{else} \end{cases} \quad (30) \\ Q_p &= \operatorname{mean}\{Q_{p,q1}, Q_{p,q2}, \dots, Q_{p,qN}\} \end{aligned}$$

where N quantile is selected and the average values are applied. For example, in 100 selected samples, each quantile is selected in step of 0.01 to obtain the accurate model of forecasting. The proposed predictive model can be used by an evolutionary algorithm such as artificial neural network to be trained and tested with actual data. To achieve this goal, multi-layer perceptron artificial neural network (MLP-ANN) has been applied to accurately predict the PV output power. The input vector to the proposed forecasting method includes temperature, humidity, dust, irradiation of solar, angle of radiation, the surface of the panel, air pressure, and the panel efficiency in energy conversion. The values of these parameters are obtained from the dataset of [35] in the one-year time interval. The updating of the weights is based on the back propagation analysis where genetic algorithm (GA) is used to achieve the optimum weights with the constraints of prediction error minimization. Using cross over and mutation in many iterations, the

optimum weights are finally obtained. In each generation of GA, the error is evaluated and checked by MLP-ANN. The forecasted PV output in each time step can be described as below:

$$P^{PV}(i+1) = P^{PV}(i) + \mathbf{w}\varepsilon_i \mathbf{x} \quad (31)$$

where \mathbf{w} is the weight vector of time-step i , ε_i is the error of this time and \mathbf{x} is the input vector. In fact, in each iteration, the calculated error is feedback to be applied in GA. The chromosomes of the genetic algorithm are selected based on neural network layers and number of neurons. This issue can be noticed in MCS strategy and the populations of genetic algorithm can be selected from the output of MCS. The characteristic of MCS in selecting different populations prevents falling the problem into the local minimum and taking the global minimum instead. Considering the QNN method, N_q samples instead of Markov model in (31) stated as below:

$$P^{PV}(i+1) = \gamma_1 P^{PV}(i) + \gamma_2 P^{PV}(i-1) + \gamma_3 P^{PV}(i-2) + \dots \quad (32)$$

$$+ \gamma_{l+1} P^{PV}(i - N_q)$$

Indeed, the total prediction process can be stated in state-space model as:

$$x(i+1) = Ax(i) + Bu(i), i = 1, 2, \dots, N_q \quad (33)$$

$$y(i) = Cx(i) + Du(i)$$

where $u(i)$ is the input parameters to the prediction system and due to iterative scheme of state space, different samples of PV can be used for prediction. The global prediction process with details is depicted in Figure 1. For error calculation, different criteria can be used as mean square error (MSE) described in below:

$$MSE = \frac{1}{m} \sum_{i=1}^m \varepsilon_i^2 \quad (34)$$

Where m denotes the iteration numbers of genetic algorithm. Through the optimization, Monte-Carlo simulation (MCS) is used to denote the uncertainties of the problem knowing that the error distribution tends to be normal distribution. Due to error probability (normal distribution) we have:

$$\mu_{pv, err} = 0 \quad (35)$$

$$E(err(i), err(i-1)) = cov(i, i-1)$$

Also in relation of correlation and variance of prediction error, we have:

$$var(err(i)) = \rho_{ii} \sigma_i^2 \quad (36)$$

where the correlation coefficient is defined as (37).

$$\rho_{i,i-1} = \frac{\sum_{k=1}^T p_{err}(i) p_{err}(i-1) - \sum_{k=1}^T p_{err}(i) \sum_{k=1}^T p_{err}(i-1)}{\sqrt{\sum_{k=1}^T p_{err}(i)^2 - (\sum_{k=1}^T p_{err}(i))^2} \sqrt{\sum_{k=1}^T p_{err}(i-1)^2 - (\sum_{k=1}^T p_{err}(i-1))^2}} \quad (37)$$

The probability of the error of prediction is presented as:

$$Prob(err_{pv}) = \frac{1}{\sqrt{2\pi\sigma_{pv}^2}} e^{\frac{-1}{2\sigma_{pv}^2}(err_{pv} - \mu_{pv, err})^2} \quad (38)$$

It must be noted that the PV model and its power generation is presented as below:

$$P_{pv} = N_{PV} \left(\frac{V_{max} I_{max}}{V_{OC} I_{sc}} \right) \left(V_{OC} - L_v(temp_{panel}) \right) irr (I_{sc} + L_i(temp_{panel}) - 30) \quad (39)$$

where L_v and L_i are the voltage and current coefficients of PV module, respectively. Considering the panel temperature, we have:

$$temp_{panel} = temp_{env} + irr \left(\frac{temp_{ave} - 25}{0.75} \right) \quad (40)$$

Considering different scenarios in panel conditions, probability of occurrence of outage and other efficient factors in PV modelling, the scenarios can be stated as summation of probabilities due to uncertainty of irradiation of solar energy and we have:

$$Sen_t = \sum_{m=1}^{N_{sc}} B_{m.t.irr} \beta_{t.irr} \cdot \rho_t \quad (41)$$

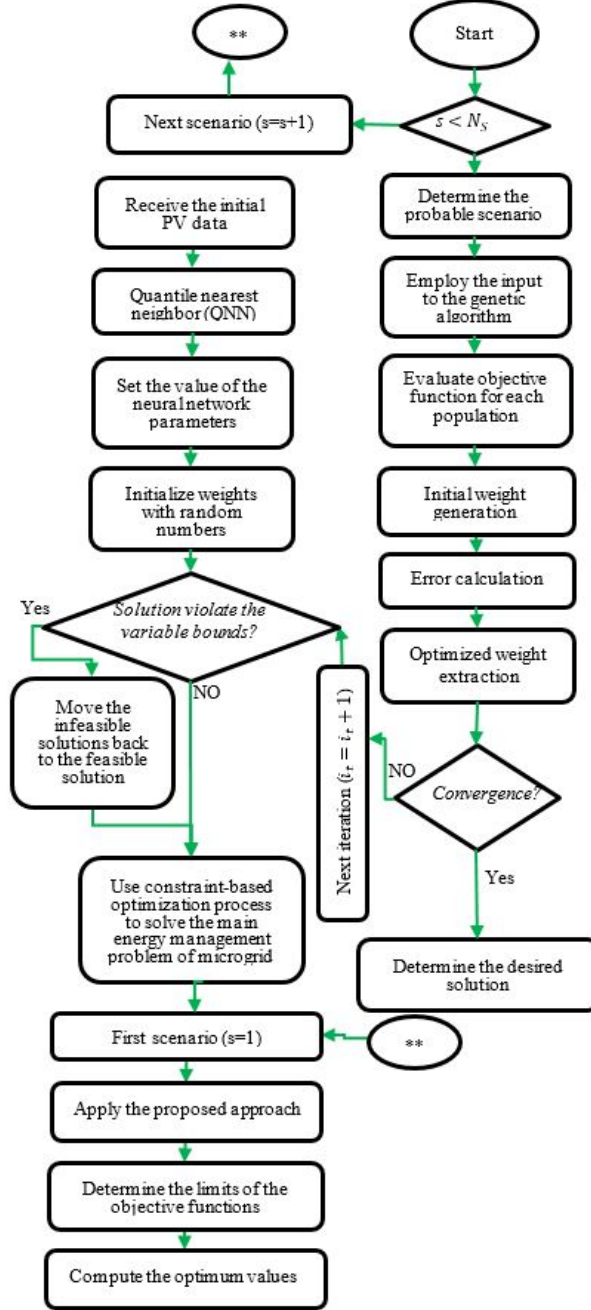


Figure 1. Flowchart of the prediction process based on QNN approach

$B_{m.t.irr}$ is the function of irradiation and $\beta_{t.irr}$ is the efficiency of irradiation transfer. ρ_t is the outage probability function defined as:

$$\rho_t = B_{t.irr}(1 - P_{out}) + (1 - B_{m.t.irr})P_{out} \quad (42)$$

Considering the input vector of MLP-ANN, the input layer of neural network includes 9 neurons, and the output layer consists of one neuron as a decision on the PV output power. For the number of neurons of hidden layer, no rigid rule exists and some papers

state the law of thumb that indicates the number of neuron in hidden layer as the average of input and output layer neurons [36]. Thus, the number of neurons of hidden layer is selected as 5. Also, lasso regression is used for testing the convergence criteria and preventing over fitting of the network. The benchmark of the proposed method is also compared with recurrent neural network in the results of prediction.

In ESS case, due to many options of buses to be selected, genetic algorithm is also used to select the suitable buses for ESS implementation. The goal is to select some buses for ESS implementation to achieve cost reduction and performance improvement. The process can be performed by the genetic algorithm simultaneously with the weight updating of MLP-ANN. Thus, using the cost function optimization, best buses for ESS implementation can be determined via GA. Note that AC power flow is executed to determine the voltage and powers of all buses before the algorithm iteration for ESS-bus selections. Power System Analysis Toolbox in MATLAB is used for this power flow [37]. The genetic algorithm flowchart is depicted in Figure 2.

4. Simulation Results and Discussion

In the system model, the per-unit power is used based on 100 KVA and the allowed range of voltage is between 0.95 and 1.05 p.u. [38]. The 24-hour profile is separated into twelve 2-hour sections and the analysis is performed for these time intervals. In this section, the model of Figure 3 is used as IEEE 15-bus microgrid for simulation tests. As shown in Figure 3, one diesel generator with capacity of 100 KVA is applied in bus 6 to support the load demand of the system. One PV generator with 150 kW rated power is also used in bus 13. 9 constant-power type loads are implemented in the microgrid and the system total active and reactive loads are 1250 kW and 380 kVA, respectively. Other data are derived from [39, 40]. The load level considered for the system is shown in Figure 4 for the one day-night in each 2-hour time step. The diagram of load level is resulted from the experimental data. The usage of ESS can control and reduce the voltage and power losses of the system. Note that the load level directly affects the storage status as, in the last part of night, the load demand is decreased and thus the storage level can be increased.

The problem of cost function in Eq. (1) is a mixed linear integer program and thus, GAMS optimization and CPLEX solver is used to solve the optimization problem. The results of applying the proposed method on the 15-bus IEEE model (test system) are obtained and discussed in this section. The result of prediction and its effect on the system cost is described in this section. Moreover, the optimal ESS implementation impact on the system performance and cost is discussed in the sequel. Note that the cost is calculated based on the data in [41] and the database for information of parameters of PV power is obtained from the 1-year dataset in [35].

Firstly, the effect of variance of prediction error is stated. As described in follow, the effect of error variance on the cost function in one-month, one-season and one-year time-period are described in Tables 2-4, respectively. As can be seen from this table, with increasing error variance, the cost of the system is increased consequently. Thus, the accuracy of prediction is an important factor in the system cost. As observable from these tables, the prediction error directly influences on the cost in different time periods. The variance of prediction exists in Eq. (1) and thus increasing the error variance causes the cost increasing consequently. Precise prediction prevents the energy wasting in the power system and provides more improvement in performance of all elements of the system.

The track property of proposed prediction method using the updated weighting steps is depicted in Figure 5. Forecasted output power is resulted from QNN and MLP-ANN using the updated weight by genetic algorithm as discussed in the previous section. As can be seen, the forecasted power desirably tracks the reference power after some iterations and error back propagation. Also, the steps of

prediction process is shown to highlight the accuracy of the proposed strategy in achieving and tracking the reference power. The result is interesting which shows that the proposed method tracks the PV power precisely with minimum error.

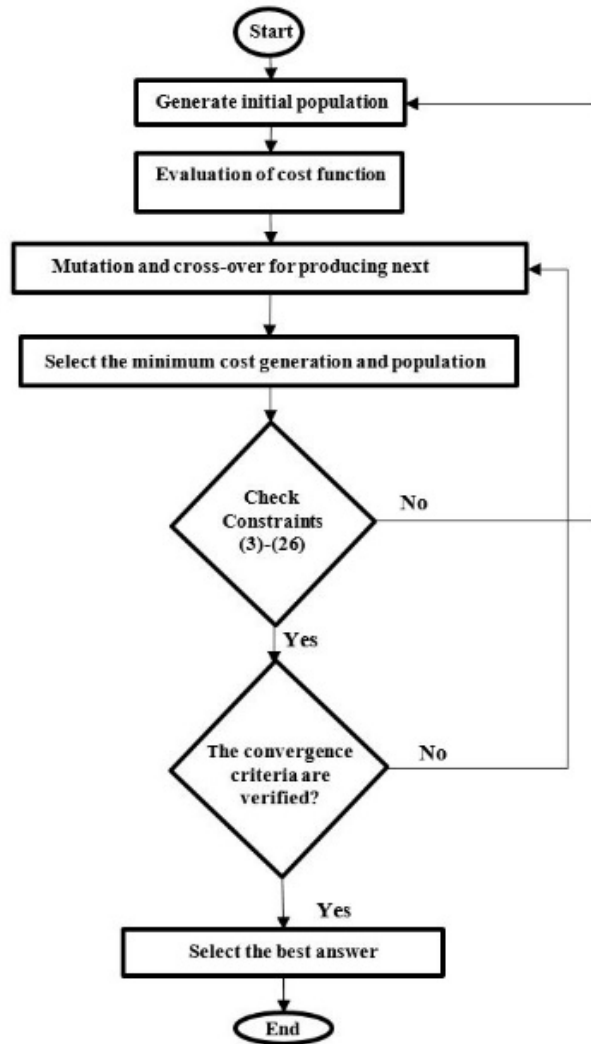


Figure 2. Flowchart of the genetic algorithm

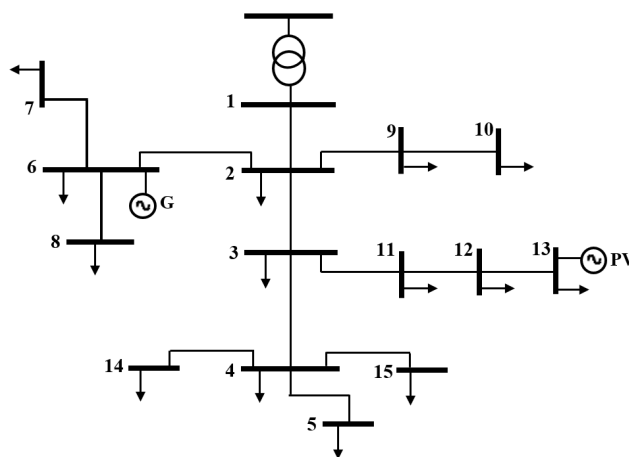


Figure 3. The IEEE 15-bus model of the microgrid

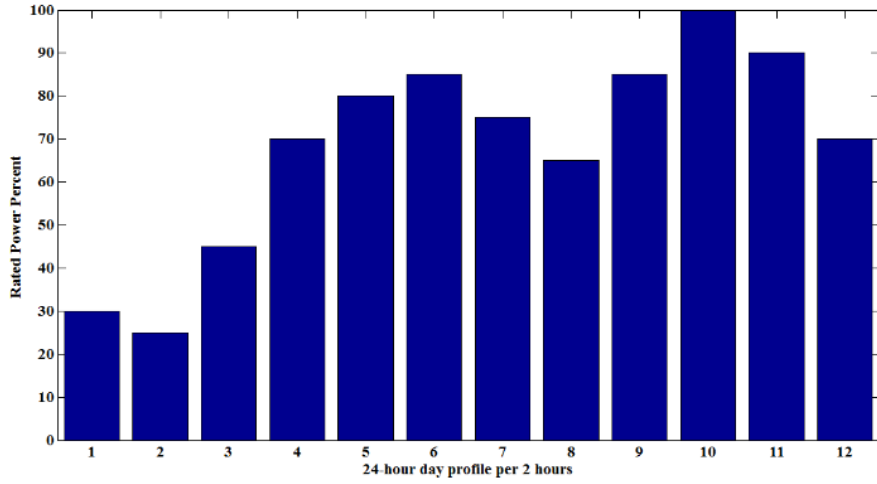


Figure 4. Load level in one-day profile

Table 2: Comparison of prediction error variances on the monthly cost of the system (by ESS implementations)

Prediction error variance (MSE)	Monthly cost (\$/month)
0.0001	231.3
0.0005	240.8
0.001	261.1
0.005	271.1

Table 3: Comparison of prediction error variances on the seasonal cost of the system (by ESS implementations)

Prediction error variance (MSE)	Seasonal cost (\$/season)
0.0001	640.1
0.0005	678.8
0.001	702.9
0.005	724.7

Table 4: Comparison of prediction error variances on the annual cost of the system (by ESS implementations)

Prediction error variance (MSE)	Annual cost (\$/year)
0.0001	2843.8
0.0005	3188.8
0.001	3400
0.005	3736

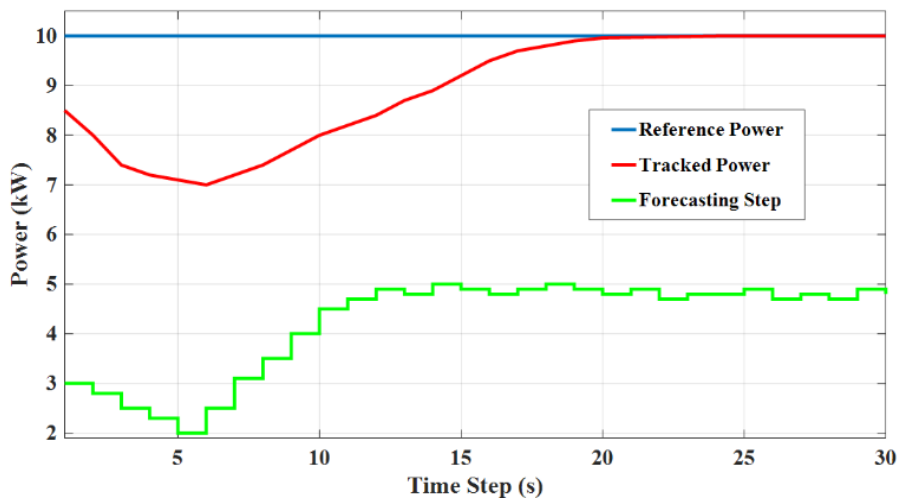


Figure 5. Track property of the proposed method related to the reference power

In the next test, the predicted PV power in different climate conditions as sunny, cloudy, overcast and rainy is depicted. As shown in Figure 6, in sunny day, the peak PV power is achievable where in cloudy day, the power variation is increased without peak power. Indeed, the uncertainty of PV power is more in cloudy day than sunny day. In the overcast and rainy days, the power peak is lost in which the maximum power occurs in two or three points without meaningful peak power.

The comparison of proposed QNN and MLP-ANN with gradient-descent ANN and recurrent neural network (RNN) is done in Table 5. In this comparison, gradient- descent and RNN are implemented as benchmarks for the verification of the proposed strategy and cost function is used for calculation of the annual cost. As described in this table, the annual cost of the proposed method with GA weight updating is less than other two similar algorithms which indicates the accuracy of the prediction process in the proposed strategy.

In Table 6, the optimum ESS location and capacity using GA is described. As described in the previous section, all buses are candidates for ESS implementation in which location and capacity of ESS are the input variables for the GA. In each iteration, GA is applied on the population of all buses and more proper buses with lower cost function are selected for the next generation. It must be noted that for better convergence of algorithm, the ESS capacity bound is limited to the range of 100-200 kWh and the number of optimum buses is set to 3. Thus, the results of Table 6 are achieved. As can be understood, the buses in the center and more cooperation with other buses are selected as the best options for the candidates of ESS implementation. Implementing the proposed ESS in the selected buses improves the performance of the power grid and voltage/power profile as will be described in the following of the paper.

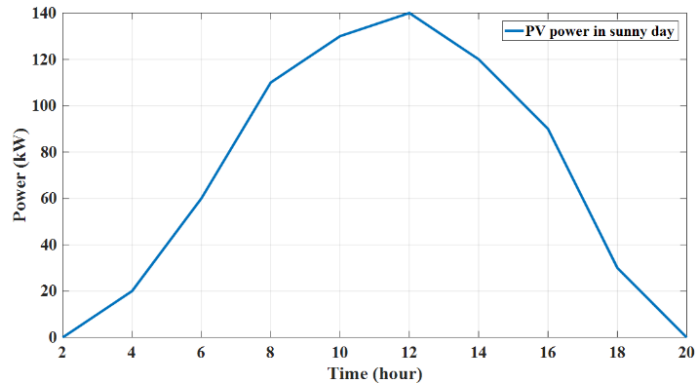
In Figure 7, the generated power is shown in two states, with and without optimal ESS deployment in the system. Optimal ESS implementation can support the load in peak time and prevent the extra power generation in the power system. It is worth mentioning that although the investment of ESS implementation and its repair cost may be high, the overall cost of the power system is reduced using the optimal ESS installation. As can be seen in Figure 7, the generated power with optimal ESS implementation in 3 selected buses (see Table 6) results in less power generation and consequently, the total cost of the power system is reduced noticeably. The analysis of Figure 7 is done based on the power generation of the proposed system in the 2-hour step of the day profile (24-hour).

Table 5: Comparison of the annual cost of the proposed MLP-ANN with gradient-descent and RNN (MSE=0.001)

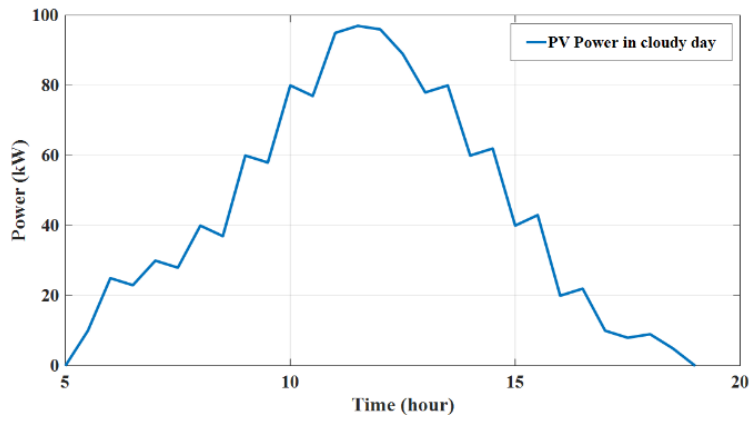
Method	Annual cost (\$/year)
Proposed MLP-ANN	3356.67
MLP-ANN gradient descent	3792.15
Recurrent neural network (RNN)	3508.42

Table 6: Optimal ESS locations, sizes and costs

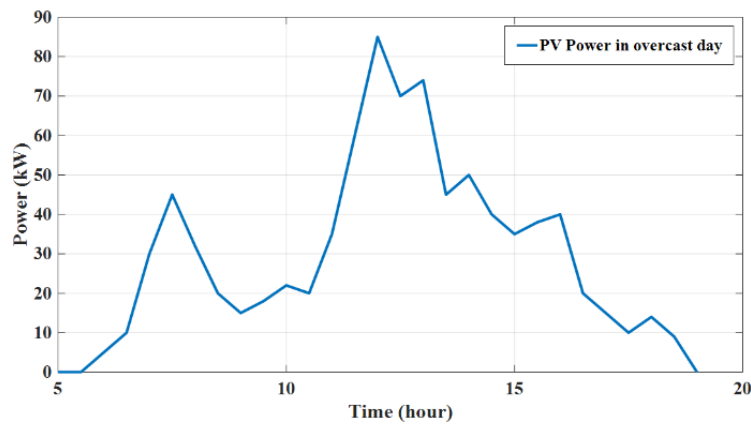
ESS number	Capacity	Location	Implementation cost (\$/year)
ESS ₁	200 kWh	bus 4	820
ESS ₂	100 kWh	bus 7	668
ESS ₃	200 kWh	bus 12	820



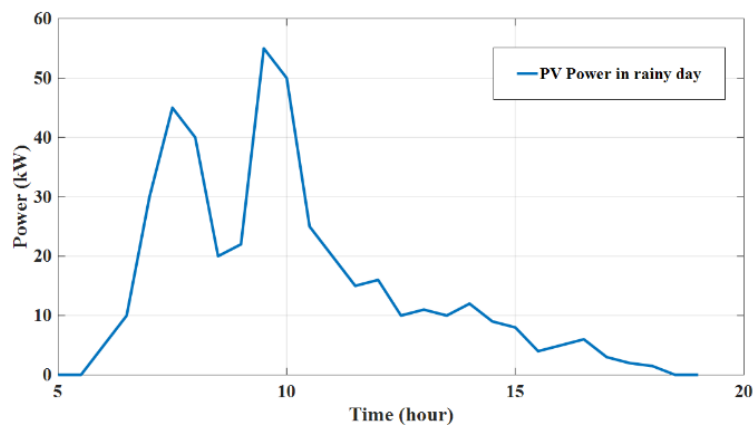
(a) Sunny day



(b) Cloudy day



(c) Overcast day



(d) Rainy day

Figure 6. Predicted PV power in different climate conditions

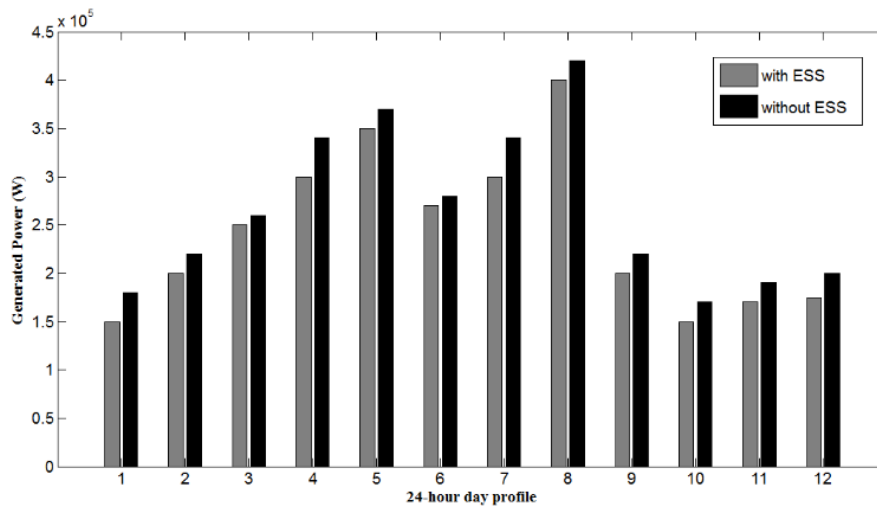


Figure 7. The generated power with and without optimal ESS implementation (analysis in 2-hour step of 24-hour profile)

In Figure 8, the generated energy with optimal ESS implementation in two cases of high and low variance of prediction error of PV output power is presented. As discussed previously, increasing the variance of prediction error causes the extra energy generation because of inaccurate prediction and thus, the cost of the system is increased. Inaccurate PV power prediction leads to more energy generation from diesel generator or more charge-discharge cycles of ESS. It is shown in Figure 8 that with low error variance, the required generated energy is less than high-error case and this shows the impact of efficient prediction on the cost of the system and energy generation.

The main goal of this paper i.e. the cost of the proposed power system is analysed in different cases and the results are reported in Table 7. Four scenarios in 1-year time period including No ESS-no PV prediction (scenario 1), No ESS with proposed PV prediction process (scenario 2), optimal ESS implementation with no PV power prediction (scenario 3), and optimal ESS installation with PV power prediction (proposed method, scenario 4) are considered in this analysis. This table shows that in the scenario 4, although prediction and ESS implementation have imposed some costs on the system, the total cost is decreased due to the energy saving of optimal ESS implementation and accurate PV prediction. It is also understood that although the effect of prediction on the total cost is less than ESS implementation, its influence on the total cost is obvious and highly noticeable in Table 7. The effect of simultaneous applying of optimal ESS and proposed PV power prediction in proposed method is obvious in this table in which the cost reduction in scenario 4 is improved as 24% and 31% compared to scenario 3 and scenario 2, respectively.

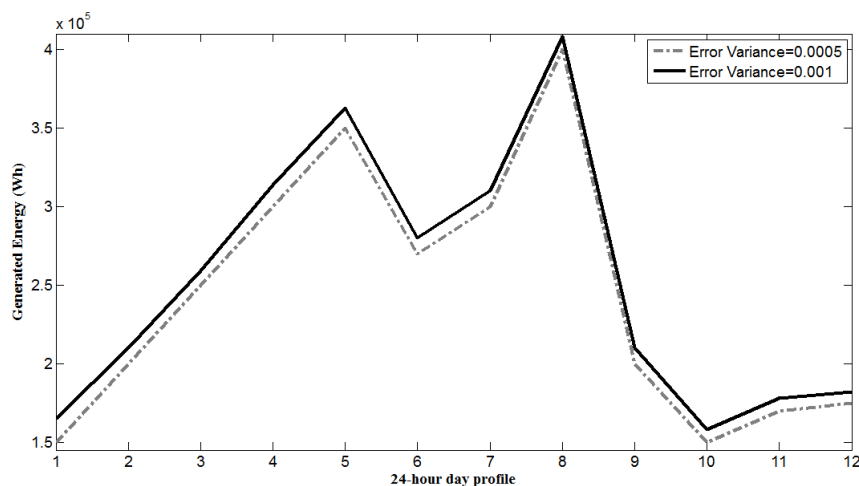


Figure 8. Total generated energy with two different variances of prediction error

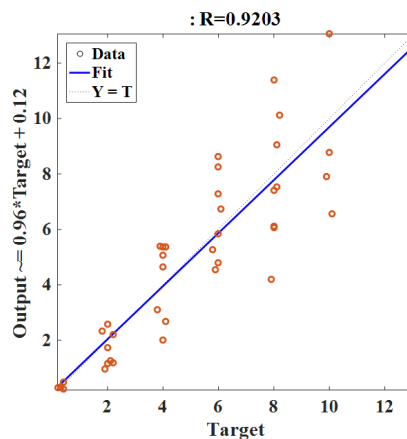
Table 7: Comparison of annual cost of different scenarios

System Model	Annual cost (\$/year)
ESS and PV prediction (scenario 4)	3377.6
ESS with no PV prediction (scenario 3)	4193.3
PV prediction with no ESS (scenario 2)	4452.1
No ESS and no PV prediction (scenario 1)	5752.2

In Figure 9, the regression diagram of proposed prediction process related to the real data of PV power is presented. As understood from this figure, the prediction accuracy is desirable and the proposed method tracks the real data which is desirable in the design of microgrid. The probability function of prediction error is normal distribution which occurs maximally in zero error with minimum variance as shown in Figure 10. Thus, the prediction error is desirably low which overcomes the bad effect of PV power uncertainty on the microgrid design and cost.

In Figure 11, the voltage profile in four scenarios is depicted. The allowed voltage range of the proposed system is between .95 to 1.05 p.u. and as can be seen in the figure, without optimal ESS and PV power prediction (scenario 4), the voltage dip or overvoltage is under or over the permitted range. However, using the proposed method in scenario 4, the voltage changes are in the desired range which results in lower power loss and performance improvement of the power grid. It is observable from this figure that using optimal ESS in the selected buses (4, 7 and 12) improves the voltage profile in these buses and adjacent buses. Moreover, the effect of PV power prediction is observable comparing scenario 2 and scenario 4 in which the voltage profile is more stable in scenario 4 and the over and under-voltage is less than scenario 2.

In view of current flow in lines of test system model (IEEE 15-bus model) shown in Figure 12, it can be seen that with the proposed method including optimal ESS installation and PV power prediction, the overcurrent and undercurrent are limited and more stability is observable in current flow. In other scenarios, the current fluctuations are seen in the lines of the model which leads to more power losses. Moreover, the current flow in lines between buses consisting of ESS is more stable and have lower changes from the nominated value. In scenario 3 (optimal ESS without PV power prediction), the current profile is more stable than the scenario 2 (PV power prediction without optimal ESS implementation) because the presence of optimal ESS in the microgrid has more important role related to PV power prediction. However, the importance of PV power prediction is observable comparing scenario 2 and 4. The improvement of the current profile of the proposed method (scenario 4) related to scenario 1, 2 and 3 is 11%, 17% and 22%, respectively.

**Figure 9. Regression of the prediction process compared with real data as target**

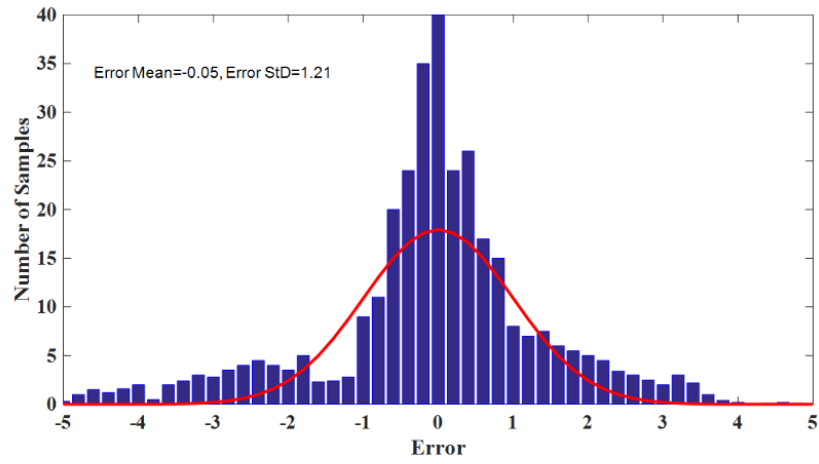


Figure 10. Probability function of the prediction error of the Proposed prediction process

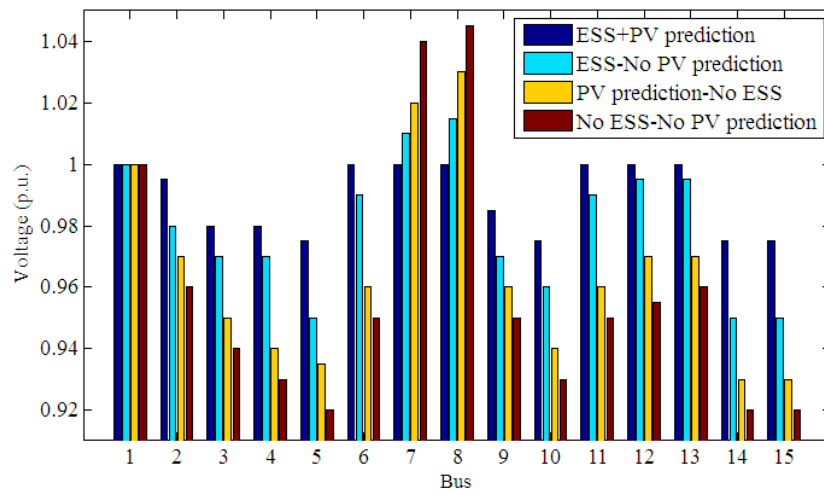


Figure 11. Voltage profile of buses in four scenarios

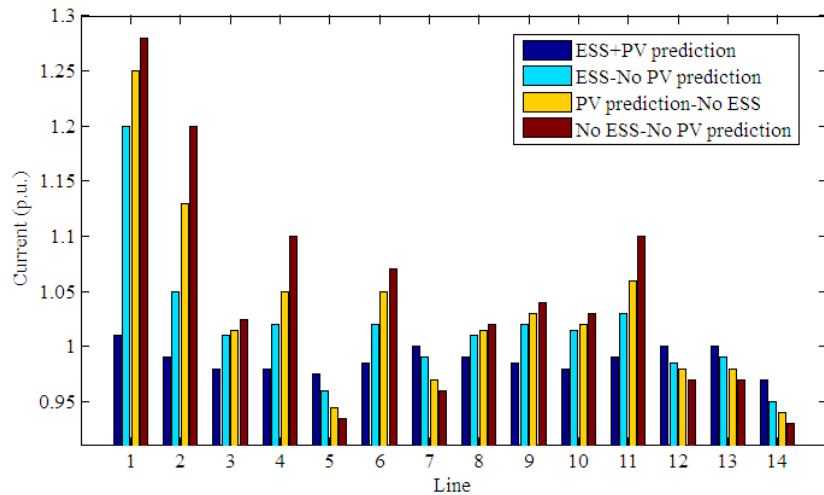


Figure 12. Current profile of lines in four scenarios

Figure 13 shows the power flow in the lines of test system model. As depicted in the figure, more fluctuations exist in scenarios 1, 2 and 3 compared to scenario 4 (proposed method) which leads to more non-stable power flow, overflow, underflow and high power losses in the microgrid. Using the proposed strategy, the power fluctuation is decreased to obtain more stable power profile. The buses of optimally implemented ESS are enhanced in power flow which verifies the effect of the optimal size and location of ESS in

the system. Also, PV power prediction gives more stability to the generated power which leads to more stable power profile. Comparing the proposed method (scenario 4) with other scenarios in view of power profile stability, it can be understood from Figure 13 that the improvement is achieved as 14%, 21% and 28% related to scenario 3, 2 and 1, respectively. In addition, in Figure 14, the effect of optimal ESS implementation compared to non-optimal ESS and No EES implementation is depicted to emphasize the proposed method efficiency in the power profile improvement.

Considering the state of charge (SOC) of implemented ESS, Figure 15 is presented to show this status in two cases of proposed PV power prediction and without that. As can be seen, the fluctuations of charge and discharge states without prediction are more than the case of using proposed PV power prediction. Moreover, without PV power prediction, the charging and discharging rate and the difference between maximum charge and discharge is higher than the case of proposed PV power prediction (see Figure 15). Discussing the correlation coefficient of prediction error, Figure 16 shows the prediction error versus the correlation factor. As observable in lower correlation factor, the prediction error is also reduced and this affects the performance of the system. Lower correlation causes lower prediction error which consequently improves the performance of the microgrid with more accurate prediction.

In the detailed prediction in time duration of a day, DG power generation and SOC of ESS in each time point are presented in Figures 17 and 18, respectively. Smaller time steps are used to obtain more accurate prediction in detail. Figure 17 shows the accuracy of power generation of each time point in the microgrid. As observable, the peak power is generated in time of 8-13 in a day. Low error between actual data and predicted one is interesting as observable from this figure. Also, Figure 18 accurately shows the status of charge and discharge of ESS in the microgrid in which, the charge state is shown in negative values and discharge is presented by positive powers. The tracking property of the proposed model is interesting observing this figure. Thus, the accuracy of proposed prediction method is verified where it causes significant improvement in the performance of the microgrid.

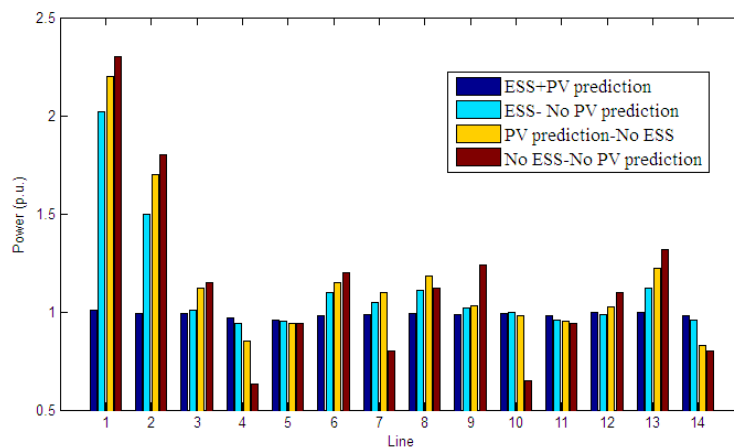


Figure 13. Power profile of lines in four scenarios

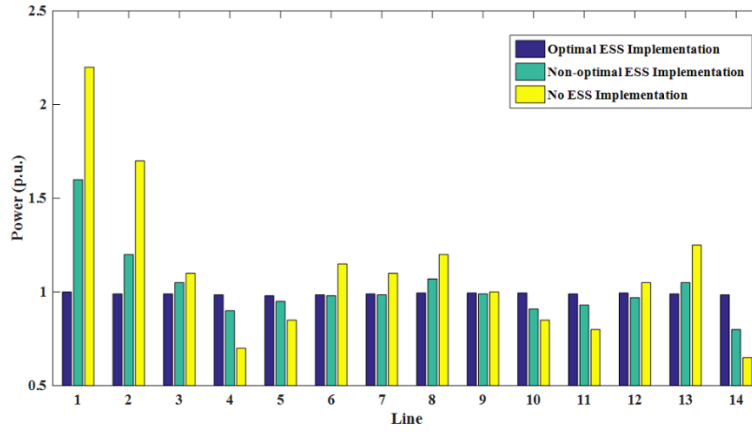


Figure 14. Power profile of lines in optimal, non-optimal and no ESS implementation

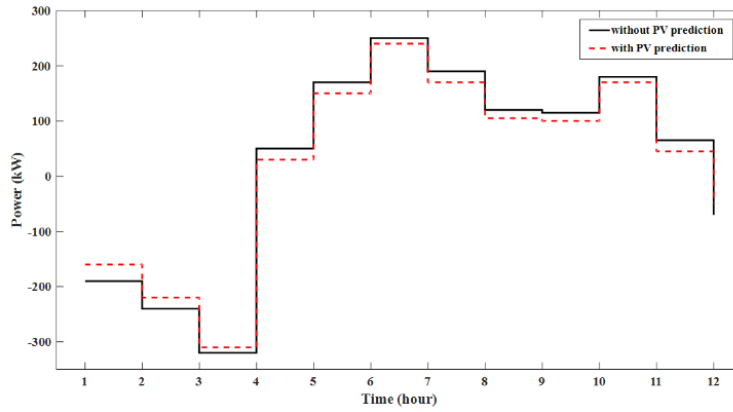


Figure 15. SOC of ESS with and without PV power prediction

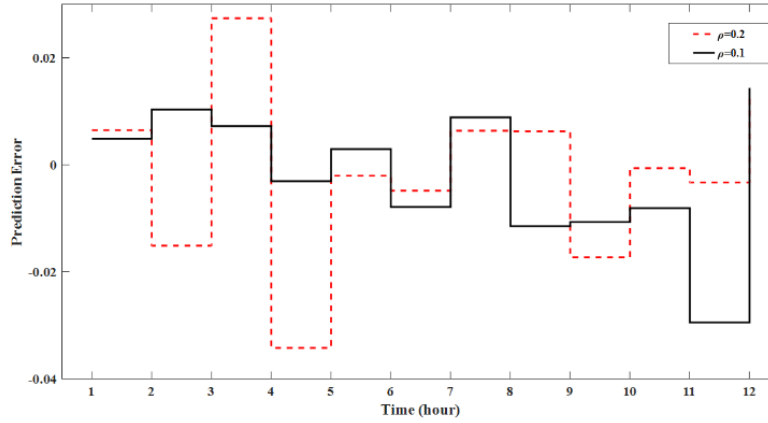


Figure 16. Effect of correlation factor on the prediction error

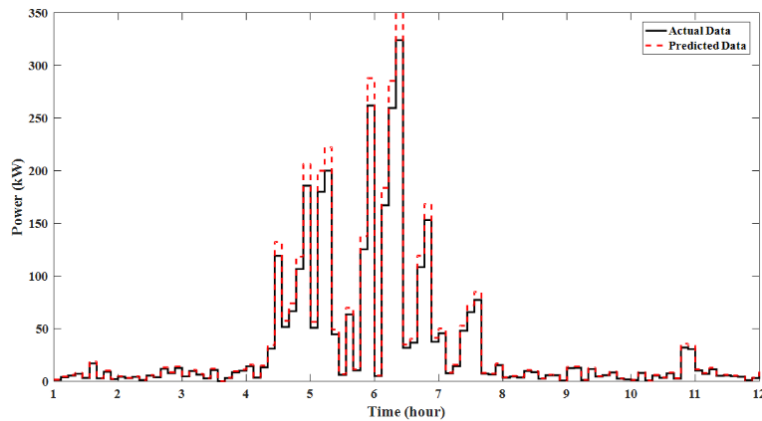


Figure 17. DG power generation in actual and predicted cases

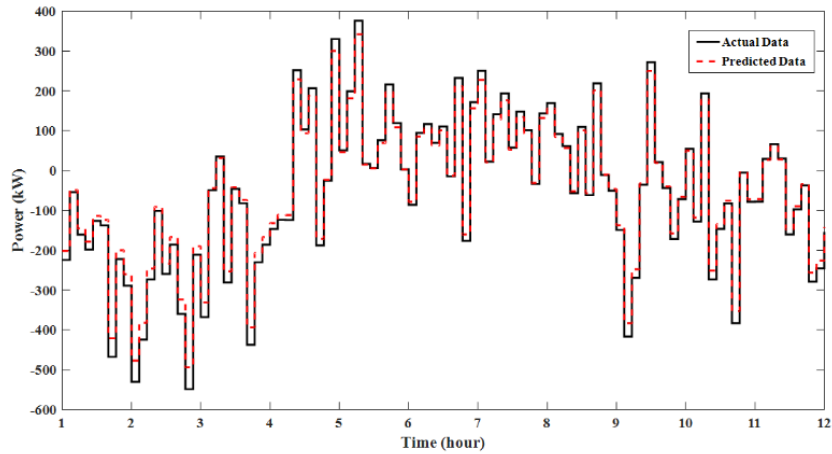


Figure 18. SOC of ESS in actual and predicted cases

5. Conclusion

This paper proposed PV output power prediction with QNN selection algorithm and applying these data to MLP-ANN and GA in addition to the optimized ESS locations and capacities to minimize the cost function in the IEEE 15-bus microgrid. Using the predicted PV output power and optimal ESS installation based on the proposed strategy, the generated power is decreased and consequently, the cost of the system is also decreased noticeably. According to the results, the cost reduction of the proposed method is enhanced by 24% and 31% relatively to the cases of optimal ESS installation without PV prediction (scenario 3) and PV prediction without optimal ESS implementation (scenario 2), respectively. The accuracy of the proposed method is more than the gradient-descent and RNN methods by about 12% and 5%, respectively. The uncertainty of PV is compensated using the proposed accurate PV power prediction, as shown in the results of this paper. The proposed method is defined as scenario 4, which improves the power profile as 14%, 21% and 28%, relatively to the scenarios 3, 2 and 1, respectively. For the future work, minimization of the cost function including green-house gases emission term can be performed using the proposed prediction strategy of PV power and optimal ESS implementation in the test microgrid.

References

- [1] W. de Carvalho, R. P. Bataglioli, R. Fernandes, D. V. Coury, "Fuzzy-based approach for power smoothing of a full-converter wind turbine generator using a supercapacitor energy storage", *Electric Power Systems Research*, vol. 184, 106287, 2020.
- [2] H. Queiroz, R. Amaral Lopes, J. Martins, "Automated energy storage and curtailment system to mitigate distribution transformer aging due to high renewable energy penetration," *Electric Power Systems Research*, vol. 182, 106199, 2020.
- [3] R. Monteiro, J. P. Bonaldo, R. F. da Silva, A. S. Bretas, "Electric distribution network reconfiguration optimized for PV distributed generation and energy storage," *Electric Power Systems Research*, vol. 184, 106319, 2020.
- [4] M. R. Djalal, M. Yunus, A. Imran, H. Setiadi, "Capacitive energy storage (CES) optimization for load frequency control in micro hydro power plant using imperialist competitive algorithm (ICA)," *Emitter Int J Eng Technol*, vol. 5, no. 2, pp. 279-297, 2018.
- [5] M. Saffari, A. de Gracia, C. Fernandez, M. Belusko, D. Boer, L. F. Cabeza, "Optimized demand side management (DSM) of peak electricity demand by coupling low temperature thermal energy storage (TES) and solar PV," *Appl Energy*, vol. 211, pp. 604-616, 2018.
- [6] J. Hu, M. Sarker, J. Wang, F. Wen, W. Liu, "Provision of flexible ramping product by battery energy storage in day-ahead energy and reserve markets," *IET Gen Trans Distribut*, vol. 12, Iss. 10, pp. 2256 – 2264, 2018.

- [7] M. Hemmati, M. A. Mirzaei, M. Abapour, K. Zare, B. Mohammadi-ivatloo, H. Mehrjerdi, M. Marzband, "Economic-environmental analysis of combined heat and power-based reconfigurable microgrid integrated with multiple energy storage and demand response program," *Sustainable Cities and Society*, vol. 69, SP. 102790, 2021.
- [8] M. Bagheri Tookanlou, M. Marzband, A. S. Al-Sumaiti, S. Asadi, B. Mohammadi-Ivatloo, A. Mohammadpour Shotorbani, A. Anvari-Moghaddam, "Energy vehicles as means of energy storage: impacts on energy markets and infrastructure," Chapter 7, *BT. Energy Storage in Energy Markets*, Academic Press, pp. 131-146, 2021.
- [9] M. Nazari Heris, M. A. Mirzaei, S. Asadi, B. Mohammadi-Ivatloo, K. Zare, H. Jebelli, M. Marzband, "Evaluation of hydrogen storage technology in risk-constrained stochastic scheduling of multi-carrier energy systems considering power, gas and heating network constraints" *International Journal of Hydrogen Energy*, vol. 45, IS. 55, pp. 30129-30141, 2020.
- [10] R. Li, W. Wang, Z. Chen, X. Wu, "Optimal planning of energy storage system in active distribution system based on fuzzy multi-objective bi-level optimization," *Journal of Modern Power Systems and Clean Energy*, vol. 6, Iss. 2, pp. 342–355, 2018.
- [11] J. G. de Matos, F. S. F. e Silva, and L. A. de S. Ribeiro, "Power control in ac isolated microgrids with renewable energy sources and energy storage systems," *IEEE Trans. Ind. Electron.*, vol. 62, no. 6, pp. 3490–3498, June 2015.
- [12] W. Shi, X. Xie, C. Chu, R. Gadh, "Distributed optimal energy management in microgrids," *IEEE Trans. Smart Grid*, vol. 6, pp. 1137-1146, 2015.
- [13] A. Gholami, T. Shekari, F. Aminifar, and M. Shahidehpour, "Microgrid scheduling with uncertainty: The quest for resilience," *IEEE Trans. Smart Grid*, vol. 7, no. 6, pp. 2849– 2858, Nov. 2016.
- [14] T.-P. DO, F. BOURRY, and X. LE PIVERT, 2017 "Assessment of Storage and Photovoltaic Short-term Forecast Contribution to Off-grid Microgrid Operation," *Proceedings IEEE PES ISGT Europe 2017*, ID 1243.
- [15] A. Ghasemi, H. Jamshidi Monfared, A. Loni, M. Marzband, "CVaR-based retail electricity pricing in day-ahead scheduling of microgrids," *Energy*, vol. 227, SP. 120529, 2021.
- [16] K. Dvijotham, M. Chertkov, and S. Backhaus, "Storage sizing and placement through operational and uncertainty-aware simulations." *Proceedings of the 47th Hawaii international conference on system science*, 2014.
- [17] H. Pandzic, Y. Wang, T. Qiu, Y. Dvorkin, and D. Kirschen, "Near-optimal method for siting and sizing of distributed storage in a transmission network," *IEEE Transactions on Power Systems*, vol.30, no.5, pp. 2288-2300, 2014.
- [18] H. Bludszuweit and J.A. Dominguez-Navarro, "A Probabilistic Method for Energy Storage Sizing Based on Wind Power Forecast Uncertainty," *IEEE Transactions on Power Systems*, vol.26, no.3, pp.1651-1658, Aug2011.
- [19] N. Gholizadeh, M. Abedi, H. Nafisi, M. Marzband, A. Loni and G. A. Putrus, "Fair-Optimal Bilevel Transactive Energy Management for Community of Microgrids," *IEEE Systems Journal*, doi: 10.1109/JSYST.2021.3066423.
- [20] M. A. Mirzaei, M. Nazari-Heris, B. Mohammadi-Ivatloo, K. Zare, M. Marzband, M. Shafie-Khah, A. Anvari-Moghaddam, J. P. S. Catalão, "Network-Constrained Joint Energy and Flexible Ramping Reserve Market Clearing of Power- and Heat-Based Energy Systems: A Two-Stage Hybrid IGDT–Stochastic Framework," *IEEE Systems Journal*, vol. 15, no. 2, pp. 1547-1556, 2021.
- [21] A. S. Al-Sumaiti, M. Salama, M., El-Moursi, M., Alsumaiti, T.S. and Marzband, M. "Enabling electricity access: a comprehensive energy efficient approach mitigating climate/weather variability – Part II" *IET Gener. Transm. Distrib.*, 13: 2572-2583, 2019, <https://doi.org/10.1049/iet-gtd.2018.6413>.
- [22] A. S. Al-Sumaiti, M. Salama, M. El-Moursi, T. S. Alsumaiti, M. Marzband, "Enabling electricity access: revisiting load models for AC-grid operation - Part I," *IET Generation, Transmission & Distribution*, 12, vol. 13, 2563-2571(8), 2019.
- [23] G. Graditi, S. Ferlito, G. Adinolfi, "Comparison of Photovoltaic plant power production prediction methods using a large measured dataset," *Renew. Energy* 2016, 90, 513–519.
- [24] H. Yang, C. Huang, Y. Huang and Y. Pai, "A Weather-Based Hybrid Method for 1-Day Ahead Hourly Forecasting of PV Power Output," in *IEEE Transactions on Sustainable Energy*, vol. 5, no. 3, pp. 917-926, July 2014.

- [25] Y. Zhang, M. Beaudin, R. Taheri, H. Zareipour and D. Wood, "Day-Ahead Power Output Forecasting for Small-Scale Solar Photovoltaic Electricity Generators," in *IEEE Transactions on Smart Grid*, vol. 6, no. 5, pp. 2253-2262, Sept. 2015.
- [26] C. Yang, A.A. Thatte, and L. Xie, Multitime-Scale Data-Driven Spatio-Temporal Forecast of Photovoltaic Generation, *IEEE Transactions on Sustainable Energy*, Vol. 6, No. 1, pp. 104-112, 2015.
- [27] H. Beltran, J. Cardo-Miota, J. Segarra-Tamarit, E. Perez, "Battery size determination for photovoltaic capacity firming using deep learning irradiance forecasts," *Journal of Energy Storage*, vol. 33, SP. 102036, 2021.
- [28] J. Lago, F. De Ridder, and B. De Schutter "Forecasting spot electricity prices: Deep learning approaches and empirical comparison of traditional algorithms", *Applied Energy*, vol. 221, pp. 386-405, 2018.
- [29] Abdel-Nasser, M. & Mahmoud, K. "Accurate photovoltaic power forecasting models using deep LSTM-RNN" *Neural Comput & Applic* (2019) 31: 2727. <https://doi.org/10.1007/s00521-017-3225-z>.
- [30] J.-F. Toubeau, J. Bottieau, F. Vallée and Z. De Grève, "Deep Learning-Based Multivariate Probabilistic Forecasting for Short-Term Scheduling in Power Markets," in *IEEE Transactions on Power Systems*, vol. 34, no. 2, pp. 1203-1215, March 2019.
- [31] Huang, C.; Bensoussan, A.; Edesess, M.; Tsui, K.L. Improvement in artificial neural network-based estimation of grid connected photovoltaic power output. *Renew. Energy* 2016, 97, 838–848.
- [32] Kazem, H.A.; Yousif, J.H.; Chaichan, M.T. Modelling of Daily Solar Energy System Prediction using Support Vector Machine for Oman. *Int. J. Appl. Eng. Res.* 2016, 11, 10166–10172.
- [33] J. F. Franco, M. J. Rider, M. Lavorato, and R. Romero, "A mixed-integer LP model for the reconfiguration of radial electric distribution systems considering distributed generation," *Electr. Power Syst. Res.*, vol. 97, pp. 51–60, Apr. 2013.
- [34] M. Shafie-khah, M. Vahid-Ghavidel, M.D. Somma, G. Graditi, P. Siano, J. P. Catalão, "IET Renewable Power Generation, 2019, Management of renewable-based multi-energy microgrids in the presence of electric vehicles, DOI: 10.1049/iet-rpg.2019.0124
- [35] <https://datacatalog.worldbank.org/dataset/iran-solar-irradiation-and-pv-power-potential-maps>.
- [36] D. Stathakis, "How many hidden layers and nodes?" *International Journal of Remote Sensing*, vol. 30, no. 8, pp. 2133-2147, 2009.
- [37] Milano F. Power system analysis toolbox (PSAT). Version 2.1.8. 2013.
- [38] Frequency Operating Standards. Australia's energy markets. 2017.
- [39] IEEE 15 Bus Radial System, <http://www.mathworks.com/matlabcentral/fileexchange/48104-ieee-15bus-radial-system>, (2017).
- [40] M. Shafie-Khah, P. Siano, D. Z. Fitiwi, N. Mahmoudi and J. P. S. Catalão, "An Innovative Two-Level Model for Electric Vehicle Parking Lots in Distribution Systems with Renewable Energy," in *IEEE Transactions on Smart Grid*, vol. 9, no. 2, pp. 1506-1520, March 2018.
- [41] S. Schoenung. Energy Storage Systems Cost Update: A Study for the DOE Energy Storage Systems Program. Technical report, Sandia National Laboratories, 2011.
- [42] S. Shi, Y. Zhang, C. Fang, Y. Wang, A. Ni and Z. Fu, "Energy Management Mode of the Photovoltaic Power Station with Energy Storage Based on the Photovoltaic Power Prediction," 2019 6th International Conference on Systems and Informatics (ICSAI), Shanghai, China, 2019, pp. 319-324.
- [43] N. Müller, S. Kouro, P. Zanchetta, P. Wheeler, G. Bittner and F. Girardi, "Energy Storage Sizing Strategy for Grid-Tied PV Plants under Power Clipping Limitations", *Energies*, vol. 12, 9, 1812, 2019.
- [44] Lee, Hyun, Kim, Gyugwang, Bhang, Byeong Gwan, Kim, David, Park, Neungsoo, Ahn, Hyung, 2018, 1, "Design Algorithm for Optimum Capacity of ESS Connected with PVs under the RPS Program," *IEEE Access*, vol. 6, DOI: 10.1109/ACCESS.2018.2865744.
- [45] Bae, Kuk Yeol, Jang, Han Seung, Jung, Bang Chul, Sung, Dan, 2019, "Effect of Prediction Error of Machine Learning Schemes on Photovoltaic Power Trading Based on Energy Storage Systems", vol. 12, DOI: 10.3390/en12071249, *Energies*.